Non-linear Dynamic Analysis with Deterministic and Random Seas: the Case of Minimum Platforms

Micaela Pilotto, University of Western Australia
School of Oil and Gas Engineering
35, Stirling Hwy
Crawley, WA 6009, Australia
micaelap@cyllene.uwa.edu.au

Beverley F. Ronalds, University of Western Australia
School of Oil and Gas Engineering
35, Stirling Hwy
Crawley, WA 6009, Australia
beverley.ronalds@uwa.edu.au

Roman Stocker, Massachusetts Institute of Technology
Dept. of Applied Mathematics
77, Massachusetts Av.
Cambridge, MA 02139, USA
stocker@math.mit.edu

***Abstract* - Minimum facilities platforms have a very simple layout and are largely used in shallow water environments. Since their natural period is four, five times smaller than the design wave period, the design is usually carried out via a quasi-static analysis amplified "a posteriori" by a dynamic amplification factor. In this paper, we investigate the limitations of this approach by comparing quasi-static and dynamic results of a non linear, time domain, finite element analysis. Three different configurations of minimum platforms are considered: one freestanding caisson and two braced monopods. We begin by investigating the response under deterministic seas, using the Stream Function formulation. We then extend the analysis to random seas, using the JONSWAP spectrum with parameters measured from the North West Shelf of Australia. The first important result is the existence of a considerable dynamic amplification under both deterministic and random seas. Interestingly, braced configurations are dynamically more sensitive than the unbraced monopod, even if the latter exhibits the largest top displacements. This can be inferred in the deterministic case from the higher values of the dynamic amplification factor. Under random waves this is further confirmed by the fact that the dynamic response of braced monopods exhibits resonant phenomena, and in particular is very sensitive to ringing. Ringing is characterized by sudden, large responses lasting for relatively short periods of time. It is shown that, among the several formulations for the dynamic amplification factor (*DAF*) in random only the one based on most probable maximum values takes ringing into account. Since so far ringing has been described mainly qualitatively in the literature, we suggest an innovative, quantitative indicator of ringing based on a careful assessment of its phenomenological properties. We are therefore in a position to quantitatively compare the ringing behavior of different structures. This analysis confirmed that braced monopods are particularly sensitive to ringing. In conclusion, we show that for design purposes the use of deterministic versus random seas as a simulation tool for the real ocean is conservative, yielding higher values of the dynamic response for all configurations. However, particular resonant phenomena, such as ringing, are not detected by a deterministic simulation.**

I. INTRODUCTION

Minimum platforms (e.g. Fig. 1) are becoming an increasingly popular solution for the development of marginal offshore oil and gas fields because of their low fabrication cost and the possibility of standardizing the design [1]. Typical structural designs for minimum platforms include free standing and braced caissons. Low levels of redundancy and greater flexibility compared with traditional offshore platforms characterize both of them. Platform dynamics may play a crucial role in the design of these structures. The natural period of minimum platforms (typically 1.5 – 2.5 sec) is usually much smaller than the period of the design wave (typically 12 – 13 sec for North Sea and Australia's North West Shelf), and this generally implies an insignificant dynamic amplification. Therefore, structural analysis is conventionally carried out using deterministic wave approach (Stokes or Stream Function, [2]) to calculate the forcing. Results from a quasi-static analysis are amplified "a posteriori" via a dynamic amplification factor, typically calculated from a single degree of freedom model. However, the nature of the hydrodynamic loading (which is drag dominated), the non-linear motion of the free surface, and the slenderness of the structures can make minimum structures extremely sensitive to loads associated with higher harmonics of the forcing wave, and therefore dynamically excitable even under waves of periods four to five times larger than the natural period of the structure. Furthermore, the dynamic amplification factor of a single degree of freedom system is smaller by up to a factor of 2.5 compared with that computed from a full dynamic analysis of these structures.

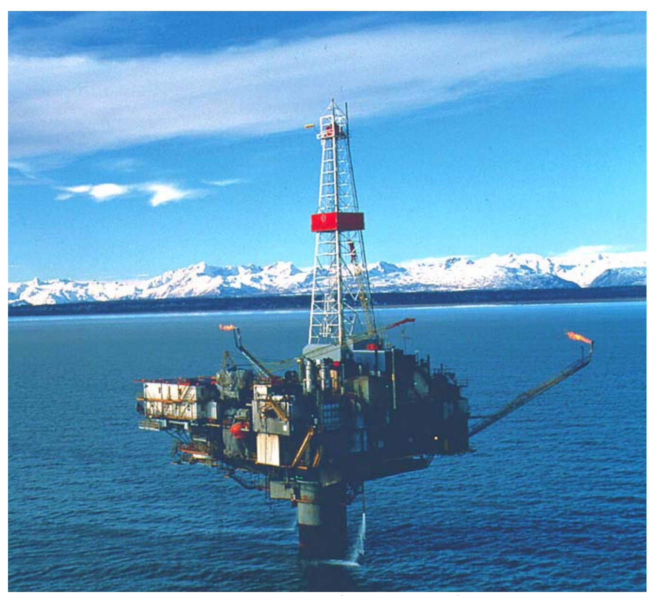

Fig. 1. A minimum facilities platform (http://www.oilandgasreporter.com/).

0-933957-31-9

II. NUMERICAL MODELS

Three different models are considered in order to compare a range of minimum structures (Fig. 2). The models have been kept simple on purpose to highlight some trends in monopod behavior. Model 1 is the most commonly analyzed single vertical cylinder, restrained at the mud-line. Model 2 is also a vertical cylinder, restrained at the height of the apex, the point where the braced substructure starts. This is to simulate a case with substantial stiff bracing below the apex. Model 3 is a simple braced monopod with the apex in the same position as Model 2. All models have the same caisson cross-section with a diameter of 1.8 m and the same material characteristics and damping ratio (ξ =1.5%). We have chosen to impose the fundamental natural period (T_n = 2.5 s) to be the same for all the models by varying the lumped mass at the top of the structure (Table I) in order to consistently compare their dynamic behavior. For a justification of the selection of these models refer to Pilotto et al. [3].

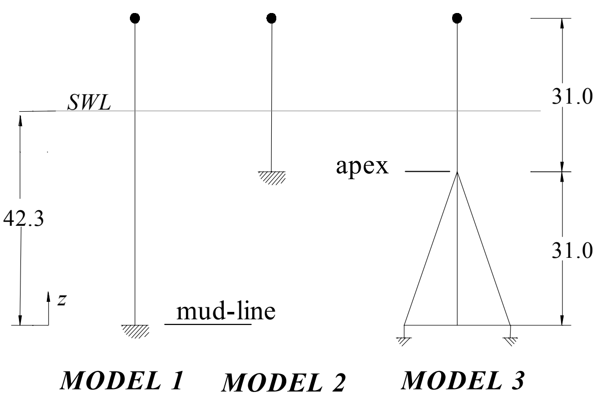

Fig. 2. Geometric characteristics of the three models.

TABLE I
MASS OF THE MODELS

	Top mass [t]	Structure mass [t]
Model 1	7.95	86.5
Model 2	220.6	43.2
Model 3	121.5	189.7

III. ANALYSIS IN DETERMINISTIC SEAS

We analyzed the behavior of minimum platforms under deterministic seas using the Stream function [2] of eighth order to simulate the sea state. The characteristics of the wave are given in Table II for the Wandoo location in Australia's North West Shelf [4]. Under these conditions the problem is non-linear. The non-linearity is due to three factors: to the wave theory (Stream function), to the quadratic relation between velocity and drag-force (the $u|u|$ term in Morison's formula, where u is the horizontal particle velocity) and to the shallow water environment (large H_w / d, where H_w is the wave height and d is the water depth). The main effects of these non-linearities are to spread the energy provided by the wave forcing over higher harmonics, therefore making these structures dynamically excitable.

A. *Dynamic Amplification factor*

In deterministic seas the dynamic amplification factor is defined as the ratio between the maximum dynamic response versus the maximum quasi-static one. Two main features are observed. First, the *DAF* increases up the water column (Fig. 3). Second, the different slopes of the three lines indicate that the dynamic sensitivity increases considerably faster up the water column for Models 2 and 3, as compared to Model 1. This is due to three reasons. The first is the stronger non-linear behavior of Models 2 and 3, best explained in terms of energy distribution (see next section). The second reason depends on the different magnitude of displacements for the three models. Since Model 1 exhibits larger displacements, and therefore velocities (the natural period being the same) than Models 2 and 3, damping plays a stronger role in the dynamic response of Model 1. The third reason is related to the different masses at the top of each structure, with the *DAF* increasing more rapidly for larger masses [3].

TABLE II
WAVE CHARACTERISTICS OF THE WANDOO LOCATION (NORTH WEST SHELF) FOR A 100 YEAR RETURN PERIOD [4]

H_w (m)	T_w (s)	d (m)
20.9	12.5	42.3

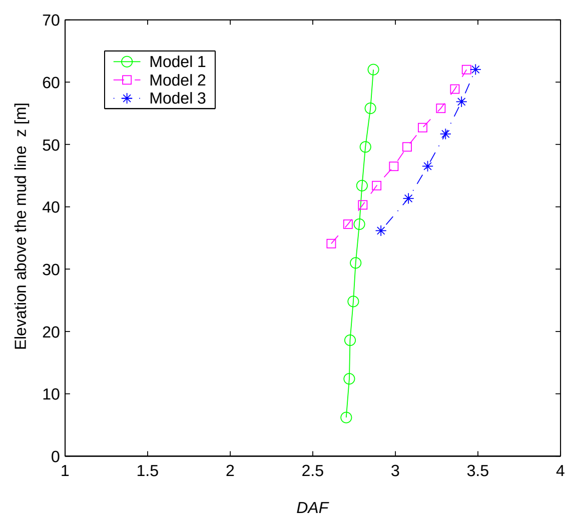

Fig. 3. Dynamic amplification factor along the water column for displacements in deterministic seas.

B. *Power Spectral Density*

The dynamic response of each configuration is compared in terms of the power spectral density of the response. We found that braced monopods (Models 2 and 3) are dynamically more sensitive than the more common analytical model of a vertical cylinder. This is explained by the fact that the power spectral density of the static response shows that Models 2 and 3 have more energy at higher frequencies than Model 1 (Fig. 4). This means that they can be dynamically excited by a wave with a period four or five times their natural period more easily than Model 1. This fact can be observed in Fig. 4. Here an energy ratio R has been computed as follows. For each model the power spectral density of the top static displacements has been normalized by its maximum static displacement. Then, for each model, R is computed as the ratio between the normalized power spectral density of the model and that of Model 1. Therefore R = 1 for Model 1. This allows to properly compare the energy of the three models for each harmonic of the fundamental forcing frequency. It is clear from Fig. 4 that Models 2 and 3, while having less energy than Model 1 at the fundamental forcing frequency, respond much more strongly to forcing at higher harmonics.

Thus, a dynamic analysis is essential for this kind of structures even if the wave frequency is very different from the first natural frequency and even if the dynamic amplification factor for the equivalent single degree of freedom structure is only marginally larger than unity.

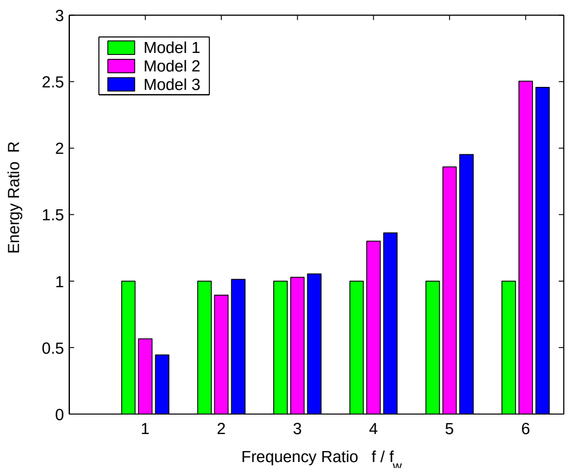

Fig. 4. Energy ratio of the three models for top static displacements.

IV. RANDOM SEAS

The behavior of the same three structural configurations has also been studied under random seas. The JONSWAP spectrum with the parameters given in Table III best represents the sea state in the North West Shelf. The results show that in random seas braced monopods can develop a peculiar resonant response known as ringing (Fig. 5). We also observe that for drag-dominated structures ringing is not only due to the non-linearity in the forcing, as reported in the literature [5], but also to the stiffness of the caisson and to the presence of a substructure, which concentrates the dynamic response in the wave zone.

TABLE III
PARAMETERS OF JONSWAP SPECTRUM FOR THE NORTH WEST SHELF FOR A 100 YEAR RETURN PERIOD [4]

H_s (m)	T_p (s)	χ	σ_a	σ_b
12.2	14.7	2	0.082	0.096

A. *Dynamic Amplification factors*

In order to obtain a practical measure of the dynamic amplification we compared two definitions of the dynamic amplification factor given in the *SNAME* report [6]. The first (DAF_1) is defined as the ratio between the standard deviation of the responses, dynamic versus quasi-static:

$$DAF_1 = \frac{\sigma_{dyn}}{\sigma_{sta}} \tag{4.1}$$

The second (DAF_2) is given in terms of the most probable maximum extremes (*MPME*) of the response, again dynamic versus quasi-static:

$$DAF_2 = \frac{MPME_{dyn}}{MPME_{sta}} \tag{4.2}$$

The *MPME* is defined as the mode value, or the highest point on the probability density function with 63% chance of exceedance. In practice this corresponds to a 1/1000 probability level in a 3-hour storm. For Gaussian processes the *MPME* can be determined analytically. In the case of non-linear, non-Gaussian processes, such as the response of minimum facilities platforms (Table IV), approximate methods are required to generate the probability density function of the process. The method proposed by Winterstein [7] and further refined by Jensen [8] fits a Hermite polynomial of Gaussian processes to transform the non-linear, non-Gaussian process into a mathematically tractable probability density function [6]. We used the method of Winterstein and Jensen, as suggested also by Yan Lu et al. [9], because it is believed to be the most efficient. In Fig. 5 DAF_1 and DAF_2 are presented for all three models as a function of the position along the water column. As observed in the deterministic case, both *DAF*s increase up the water column, showing that the dynamic response is enhanced in the wave zone, particularly for Models 2 and 3. In both deterministic and random seas the unbraced model (Model 1) exhibits the weakest dynamic amplification: the dynamic amplification factor is the smallest of the three models and does not increase significantly up the water column. Models 2 and 3, on the other hand, show in both cases to be dynamically sensitive. The values of both *DAF*s are smaller than those in the deterministic case for both displacements and bending moments. This is because the deterministic analysis is intrinsically more conservative, in the sense that velocities and accelerations calculated for the deterministic case are larger than those measured in the field and therefore the loads on the structure and the structural response are larger. This is evident particularly for Models 2 and 3 in the wave zone.

Interestingly, while in the deterministic case Model 3 has the largest *DAF*, in random seas Model 2 exhibits the largest value. This is because in random seas the resonant behavior is enhanced, with ringing phenomena lasting for a long time, in the orders of minutes (Fig. 6). This behavior is not noticed in deterministic seas and greatly influences the magnitude of the dynamic amplification factor. Another feature that can be observed from Fig. 5 is that the values of DAF_2 are larger than those of DAF_1, particularly for Models 2 and 3. Taking average values over the water column, for Model 1 DAF_2 is larger than DAF_1 by about 10%, for Model 2 by 13% and for Model 3 by about 30 %. This difference can be attributed to ringing. This can be explained by the fact that ringing is a transient event lasting for short periods of time and does therefore not significantly influence the standard deviation of the response and thus DAF_1. On the other hand, DAF_2 is more sensitive to extreme values, because it is defined in terms of *MPME* values, and is thus more suitable to detect ringing. Therefore, in random seas the two *DAF*s, which could be at first considered apparently equivalent (since both capture the increase in the dynamic over the quasi-static response), are in fact different in the case that transient events, such as ringing, occur.

On the other hand, while DAF_2 can detect the dynamic amplification produced by short, temporally localized resonant events, it does not give any indication about the kind of amplification occurring. For example it cannot distinguish between springing, ringing or other resonant effects. This prompted us to define some indicators in order to specifically identify ringing events, as described in the next section.

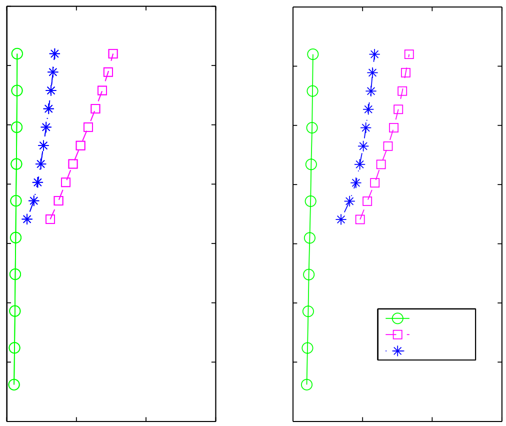

Fig. 5. Dynamic amplification factors (DAF_1 and DAF_2) in random seas for the top displacements of the three models up the water column.

A. Ringing

Ringing was first identified in the early 1980's in Hutton's tension leg platform model tests [10]. This resonant phenomenon is associated with large, steep waves and it has been observed to contribute significantly to the response of large-volume fixed and floating platforms [11]. Therefore, studies have focused so far mainly on large-volume structures, which are dominated by inertia and are minimally affected by drag forces ([12], [13]). However, tests performed by Sterndorff and Thesbjerg [14] showed that monopods, with a natural period ranging between 2 and 4 s, also respond dynamically to wave loading and, under certain conditions (transient, very steep waves), exhibit ringing. Moreover Nedeergard et al. [5] observed ringing in a braced monopod, suggested the higher harmonics in the wave loading to be the cause. The effects of ringing on drag-dominated structures have never been thoroughly investigated [15], despite the potential importance of ringing from the structural point of view, in particular with respect to increased loads and fatigue [16]. Furthermore, the fact that the bending moments on the upper part of the caisson are amplified by ringing, is of interest in view of the fact that the failure of the Campbell monopod [17] occurred in the wave zone. Our approach will be twofold. First, we will define three ringing indicators, in order to be able to compare the effect of ringing on the three models. Second, we will reinterpret their quasi-static and dynamic response in light of those indicators.

1) Phenomenological Characteristics of Ringing

A Gaussian distribution is the frequency distribution of many natural phenomena and its graph is the well known bell-shaped curve. This curve is symmetric with respect to the mean and has skewness equal to zero and kurtosis equal to four. It is also known that ocean waves can be modeled as a linear random superposition of sinusoidal waves, which are entirely described by the wave spectrum. The statistics of the underlying random process are Gaussian. On the other hand, the free surface effects together with the fact that drag forces introduce non-linearities in the wave kinematics, make the hydrodynamic forcing always non linear. As a result, the random excitation is non-Gaussian and the response of the drag-dominated structures is therefore also non-Gaussian. This can be seen from the parameters given in Table IV for the top displacements of the three models. In particular skewness and kurtosis have very high values. However, these parameters by themselves do not capture the presence of ringing, as suggested by [12] among others. Indeed, Models 1 and 3 have both the largest values of skewness and kurtosis, but it is Models 2 and 3 that exhibit ringing, while Model 1 does not. Clearly another way of quantifying ringing must then be found.

TABLE IV

STATISTICAL PARAMETERS OF THE DYNAMIC RESPONSE OF THE TOP DISPLACEMENTS FOR THE THREE MODELS. THE SECOND COLUMN INDICATES THE RANGE OF VALUES ASSUMED BY THE PARAMETERS IF THE RESPONSE WERE GAUSSIAN. CLEARLY ALL THREE MODELS BEHAVE IN A NON-GAUSSIAN FASHION.

Parameters	Gaussian response	Model 1	Model 2	Model 3
μ (mean)	0	0.0323	0.0018	0.0044
σ (std. dev.)	$0.25H_s \pm 1\%$	0.2630	0.0180	0.0255
α_3 (skewness)	-0.03 ÷ 0.03	1.94	0.68	2.23
α_4 (kurtosis)	2.9 ÷ 3.1	14.79	6.81	21.08

Ringing is usually characterized by a sudden, strong amplification in the response. The initial peak, much larger than the previous oscillations, is then followed by a number of slowly decaying peaks. A typical event can be seen in Fig. 7, bottom panel. We can quantify this by saying that there is a ringing event when all three of the following criteria are verified:

1. The first peak is much larger than the average magnitude of all peaks. The latter can be taken to be proportional to the standard deviation of the response, with a proportionality factor K. This reflects the fact that ringing is indeed characterized by a strong amplification of the response. With this criterion we consider as ringing phenomena only those peak responses that are considerably larger than an average response.

2. When a peak obeys criterion one, the following peaks must be smaller than the first one and they must be in a large enough number (N_{foll}). This criterion captures the slow logarithmic decay after the first, large peak which is typical of ringing.

3. A certain number of peaks (N_{prec}) preceding the first one must be considerably smaller than the first peak, in order to have the sudden start which is characteristic of ringing. In particular, we chose to require those N_{prec} peaks to have less than half the amplitude of the first one. This criterion reflects the suddenness of initiation of ringing.

The values of these parameters (K, N_{foll}, N_{prec}) need to be chosen. We have taken K = 4, N_{foll} = 6, N_{prec} = 5. A MATLAB routine has been written in order to automatically detect ringing events for a given time series (Figs. 6 and 7). While there is admittedly a certain degree of freedom, and therefore subjectivity, in our choice of the parameters, there is no doubt that once a set of parameters has been picked, comparison among different ringing events becomes quantitative and objective. Furthermore, the above values were carefully chosen after a prolonged tuning exercise so as to identify as ringing events those and only those events which most naturally appear as such by visual inspection of the time series. The difference with several previous qualitative descriptions of ringing resides in the fact that we have been able to translate the phenomenological characteristics of ringing in simple and yet objective criteria, allowing quantitative prediction of the ringing behavior for different models and different conditions.

2) Ringing Indicators

The criteria introduced in the previous section allow us to detect ringing events in a time series. To extract quantitative information from this result, some synthetic parameters must be computed. Three indicators have been identified as important in characterizing a ringing response: the first is simply the number (N_R) of ringing events that occur in a time series. The second (m_R) is a measure of the average amplification that occurs during a ringing event. This is defined as the average of the maximum value of each event divided by the standard deviation of the whole time series. The third (M_R) captures the maximum value of the amplification exhibited by the structure. It is calculated as the ratio of the maximum ringing peak and the standard deviation of the entire response. In Table V the values of these three parameters are given for the three models for both, apex bending moments and top displacements. It can be seen that the indicators reflect the behavior of the models, which we previously described only in a qualitative fashion. In fact, ringing is almost absent for Model 1. In this case, with only one event characterized as ringing for the bending moments (N_R = 1) and none for the top displacements, the values of m_R and M_R are not representative. On the other hand, Models 2 and 3 are comparable. They have approximately the same number of ringing events for both, top displacements and apex bending moments. However, Model 3 has larger values of m_R and M_R than Model 2. This is interesting because, as we have seen in the previous section, the dynamic amplification factors attained by Model 2 are larger. However, Model 3 experiences stronger and more sudden ringing, as indicated by m_R and M_R.

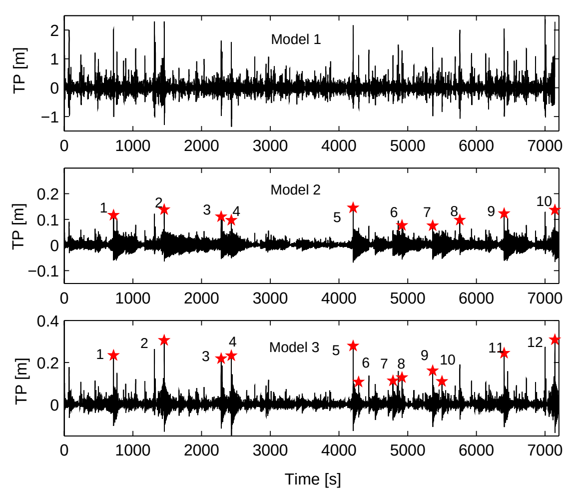

Fig. 6. Ringing in the top dynamic displacements (TP) for a two-hour simulation. The stars characterize the start of a ringing event as defined in the text and ringing events are numbered progressively. Models 2 and 3 exhibit ringing, Model 1 does not, despite its larger amplitudes (note the different vertical scale).

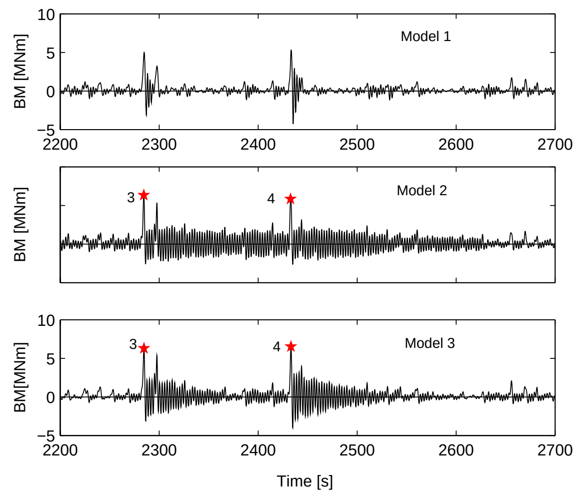

Fig. 7. Ringing in the bending moments at the apex (BM) for a two-hour simulation. The stars characterize the start of a ringing event as defined in the text and ringing events are numbered progressively. A close up on events 3 and 4 is shown.

TABLE V
RINGING INDICATORS FOR APEX BENDING MOMENTS (BM) AND TOP DISPLACEMENTS (TP) FOR THE THREE MODELS DURING A TWO-HOUR SIMULATION.

	Model 1		Model 2		Model 3	
	BM	TD	BM	TD	BM	TD
N_R	1	0	9	10	11	12
m_R	11.2	0	7.4	6.2	8.4	8.0
M_R	11.2	0	9.2	8.0	12.2	12.1

B. *Power Spectral Density*

In order to explore how the dynamic response influences the energy of the monopods, we computed the power spectral density of the dynamic. In Fig. 8 the power spectral density of the dynamic top displacements is compared among the three models. Also included in the comparison is the spectrum of the wave elevation. Model 1 has a larger amount of energy because it exhibits the largest top displacements. The largest peak is at the same frequency (0.07 Hz) as the peak frequency of the wave elevation and it is due to direct wave forcing. Models 2 and 3 have less energy (smaller top displacements) but at the frequency of 0.4 Hz (first natural mode) they exhibit a sharp increase in the power spectral density, which reaches values close to those of Model 1. This is again due to ringing, which amplifies the response at the natural frequency and therefore increases significantly the energy density at 0.4 Hz.

A closer look at the peaks at 0.4 Hz shows that Model 2, which overall has less energy than Model 3, overcomes the energy of Model 3 at the natural frequency. This is due to the fact that Model 2, being stiffer, overall exhibits smaller displacements than Model 3, but when ringing occurs the amplification is larger than that of Model 3.

In order to compare the overall energy of the three models, the integral of the power spectral density, representing the total energy in the response, has been calculated for the quasi-static and dynamic cases. The ratio of the total dynamic and the total quasi-static energies, reported in Table VI, can be considered as another index of the dynamic amplification, whose physical meaning is close to that of the dynamic amplification factor. In Fig. 9 this energy ratio is plotted for each node of the structures along the water column. The behavior of the total energy ratio is surprisingly similar to that of the dynamic amplification factors seen previously (Fig. 5). Like the dynamic amplification factor, the total energy for Model 1 is smallest and increases only slightly up the water column. Model 2, on the other hand, has the largest total energy, strongly increasing up the water column, due to its resonant behavior and its large stiffness. Model 3 shows an intermediate behavior, as it did in terms of the dynamic amplification factors.

In order to further investigate how the power spectral density varies along the water column and how the two main peaks contribute to the total energy in the upper part of the structure, the power spectral density for the displacements of Model 3 has been plotted in Fig. 10 as a function of the vertical position along the water column starting from the apex up. It can be seen that the strength of the peak at 0.4 Hz increases up the water column (larger values of z), showing even more clearly that the dynamic response is enhanced in the upper part of the structure. Fig. 11 shows the same plot, but for the bending moments. In this case, looking more closely at the low frequencies, it can be observed that the first peak (the one at 0.07 Hz), due directly to wave forcing, decreases dramatically going up the water column. This is best seen in Fig. 12, where the first peak (at 0.07 Hz) and the second peak (at 0.4 Hz) are plotted along the water column. The fact that the energy decreases up the water column is coherent with the general behavior of the bending moments, which are greater at the apex for Model 3 and decrease upwards. However, up in the water column the “ringing” peak at 0.4 Hz still retains a considerable amount of energy, comparable with the energy at the apex.

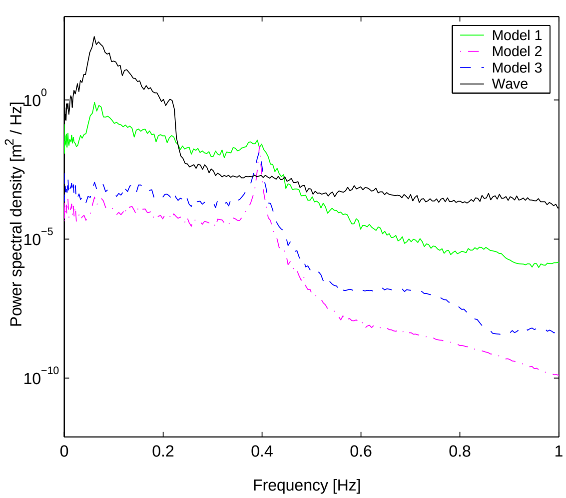

Fig. 8. Power spectral density of the dynamic top displacements for the three models. Also shown is the power spectral density of the wave elevation.

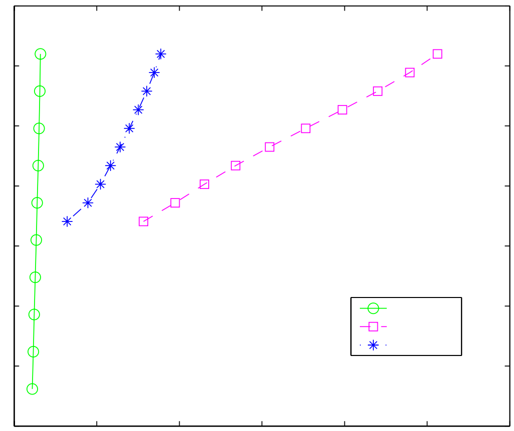

Fig. 9. Ratio of the total dynamic energy and the total quasi-static energy along the water column for the three models. Both energies are calculated as the integral of the power spectral density from Fig. 8. Compare with the dynamic amplification factors in Fig. 5.

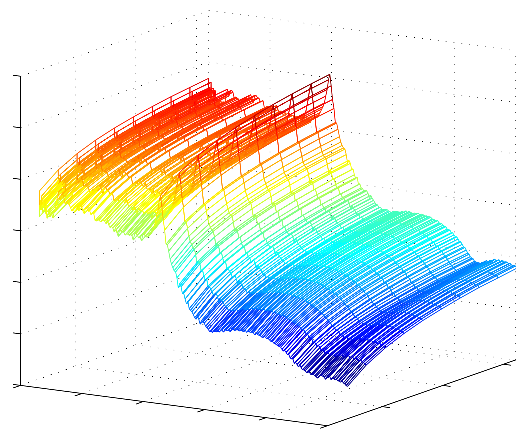

Fig. 10. Power spectral density of the displacements of Model 3 for each node along the water column.

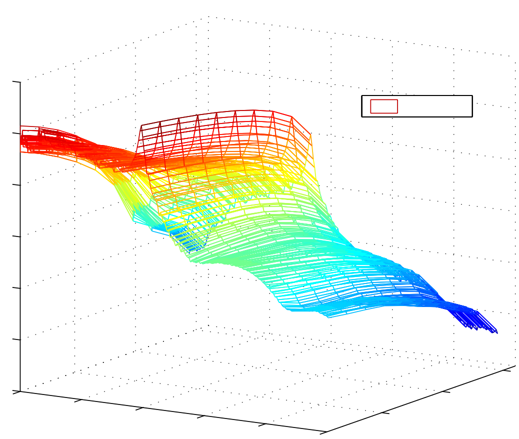

Fig. 11. Power spectral density of the bending moments of Model 3 for each node along the water column.

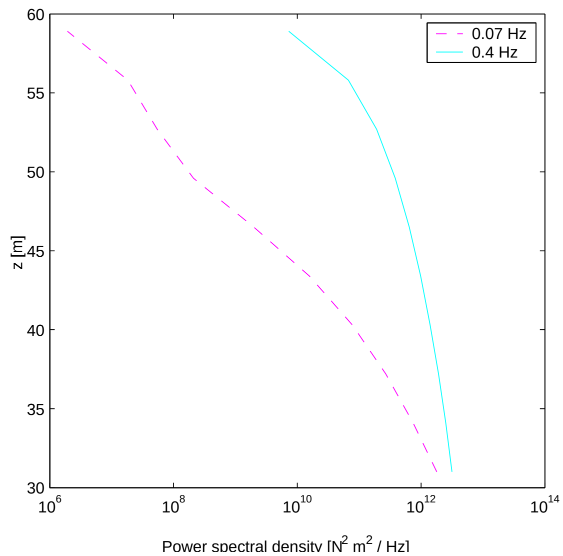

Fig. 12. Power spectral density of the bending moments for Model 3 along the water column for the first peak (at 0.07 Hz) and the second peak (at 0.4 Hz).

V. COMPARISON OF BENDING MOMENTS

Since the design of minimum structures is generally governed by bending moments, it is interesting to compare the dynamic bending moments under random seas, and in particular their most probable maximum values, with the quasi-static deterministic moments amplified by the dynamic amplification factor of a single degree of freedom model (DAF_{SDOF} = 1.05), which is used in the design practice. In Fig. 13 these values are compared. As expected, the design moments (deterministic quasi-static amplified by DAF_{SDOF}) are larger than those found with the random seas dynamic analysis. This indicates that, in general, the design is conservative. However, while the ratio between deterministic quasi-static and random dynamic moments is large at the base (Model 1) or at the apex (Models 2 and 3), higher up in the water column this value becomes smaller, thereby decreasing the safety margin in the wave zone. This is clearly shown in Fig. 14, where the ratio of the bending moments presented in Fig. 13 is plotted. It can be noted that, while the ratio increases up the water column for Model 1 reaching values of seven or more, for the braced configurations (Models 2 and 3) the ratio decreases fast to values as low as 1.5.

Since in the design practice other factors intervene, namely the presence of internal conductors and risers and installation requirements, usually the caisson's cross section is constant along the water column for economical and practical reasons and is able to withstand the upper bending moments. Therefore, the fact that bending moments under random seas decrease more slowly up the water column than design values should not in general be a concern for safety. However, a more optimized design would suggest taking advantage from two facts. First, that bending moments are actually smaller than those predicted with a deterministic quasi-static analysis. Second that their decrease along the water column is by no means as fast as predicted in the quasi-static deterministic case. Furthermore, while the usual design practice is in general conservative, the above argument suggests a possible explanation of what have contributed to the failure of the Campbell monopod in the wave zone. A reduced safety margin of the random dynamic versus the design quasi-static moments, possibly coupled with additional factors, may have been the case for this failure.

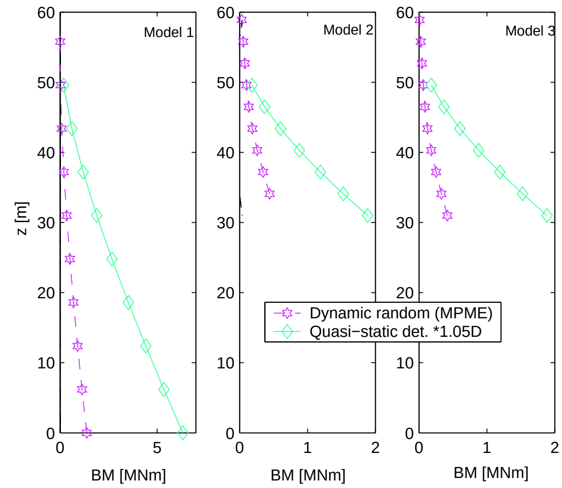

Fig. 13. Comparison of quasi-static bending moments obtained with the deterministic wave and amplified by the dynamic amplification factor of a single degree of freedom model (DAF_{SDOF} = 1.05) and dynamic bending moments (most probable values) obtained with random sea simulations. The quasi-static response was calculated using the Stream function of order eighth.

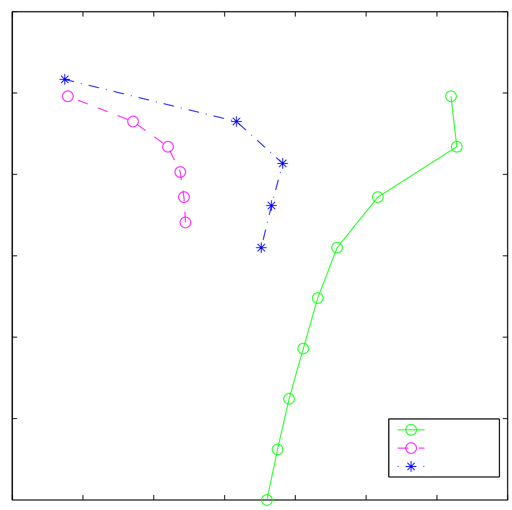

Fig. 14. Ratio between quasi-static bending moments obtained with the deterministic wave and amplified by the dynamic amplification factor of a single degree of freedom model (DAF_{SDOF} = 1.05) and dynamic bending moments (most probable values) obtained with random sea simulations.

VI. CONCLUSIONS

In this paper, we performed a non-linear, time domain, finite element analysis of three different configurations of minimum platforms. We first investigated the response under deterministic seas, using the Stream Function formulation. We then extended the analysis to random seas, using the JONSWAP spectrum. The parameters used in both cases are for the North West Shelf of Australia. We found that minimum structures, which typically are designed using the quasi-static results amplified with the dynamic amplification factor for a single degree of freedom model, are strongly dynamically sensitive in both deterministic and random seas. Our study shows that braced and unbraced structures perform very differently, with the braced configurations being dynamically more sensitive than the unbraced ones, even if the latter exhibit larger top displacements.

Ringing has been identified as the main feature of the random sea analysis of the braced models for bending moments and displacements. It has been shown that in general two parameters can detect the dynamic amplification due to ringing, namely the dynamic amplification factor defined in terms of *MPME* and the ratio of the dynamic and quasi-static total energies. However, since these parameters are not able to recognize the kind of resonance causing the amplification in the response, we defined three indicators in order to specifically identify a ringing event. Results show that Model 3 is the one most affected by ringing.

Since the structural analysis of minimum platforms is conventionally carried out using deterministic waves to calculate the forcing and adopting a quasi-static analysis amplified by the dynamic amplification factor for the single degree of freedom model, we compared these results with those of a non-linear dynamic analysis in random seas. Our conclusions show that for design purposes, the use of deterministic versus random seas as a simulation tool for the real ocean is conservative, yielding higher values of the dynamic response for all configurations. However, particular resonant phenomena, such as ringing, are not detected by a deterministic simulation and the safety margin of the design values decreases strongly in the wave zone.

ACKNOWLEDGMENT

This work was undertaken as part of a research project within the Cooperative Research Centre for Welded Structures (CRC-WS), whose support is gratefully acknowledged. The entire project has been possible thanks to an International Postgraduate Fee Exemption Scholarship and a University of Western Australia Postgraduate Award. A particular thank you to Dr. Geoff Cole, whose detailed comments are always greatly appreciated.

REFERENCES

[1] E.K. Albaugh, P. O'Connor, and B. Robinson, "Oil and gas prices, new concepts, technology renew interest in minimal facilities", *Offshore*, vol. 61, no.1, pp. 58-60, February 2001.

[2] R.G. Dean, "Stream function representation of nonlinear ocean waves", *J. of Geophysical Research*, vol. 70, no.18, pp. 4561-4572, 1965.

[3] M. Pilotto, B.F. Ronalds and R. Stocker, "Dynamic response of shallow water monopod platforms", *Proc. 21st Int. Conf. OMAE*, ASME, Oslo, Norway, 2002.

[4] Steedman Science & Engineering, *Oceanographic and meteorological design criteria – Wandoo location*, Report R590, 1994.

[5] H. Nedergaard, J. Tychsen and S. Lyngesen, "Ringing and double frequency response of a tripod", *Proc. 16th Int. Conf. OMAE*, ASME, vol. 1, part A, pp. 497-505, 1996.

[6] SNAME, "Guidelines for site specific assessment of mobile jack-up units", Society of Naval Architects and Marine Engineers, *Technical and Research Bulletin 5-5A*, Rev 1, New Jersey, 1997.

[7] S.R. Winterstein, "Nonlinear vibration models for extremes and fatigue", *J. Engrg. Mech.*, ASCE, vol. 114 (10), pp.1772-1790, 1988.

[8] J.J. Jensen, "Dynamic amplification of offshore steel platform response due to non-gaussian wave loads", *Marine Structures*, vol. 7, pp.91-105, 1994.

[9] Y. Lu, Y.N. Chen, P.L. Tan and Y. Bai, "Prediction of jack-up dynamic response", *Proc. 20th Int. Conf. OMAE*, ASME, Rio de Janeiro, Brazil, 2001.

[10] J.A. Mercie, "Evolution of tension leg platform technology", *Behavior of Offshore Structures*, Boston, 1982.

[11] K.B. Davies, S.J. Leverette and M.W. Spillane, "Ringing response of TLP and GBS platforms", *Proc. 7th Int. BOSS Conf.*, pp. 587-605, Boston, 1994.

[12] E.R. Jefferys and R.C.T. Rainey, "Slender body models of TLP and GBS ringing", *Proc. 7th Int. BOSS Conf.*, pp. 569-585, Boston, 1994.

[13] B.J. Natvig, "A proposed ringing analysis model for higher order tether response", *Proc. 4th Int. Conf. ISOPE*, 1994.

[14] M.J. Sterndorff and L. Thesbjerg, "Experimental investigation of monotower platform dynamics", *Proc. 16th Int. Conf. OMAE*, ASME, vol. 1, part A, pp. 165-173, 1996.

[15] N. Spidsøe and D. Karunakaran, "Effects of non-gaussian waves to the dynamic response of jack-ups platforms", *Marine Structures*, vol. 10, pp. 131-157, 1997.

[16] J. Grue, "On four highly nonlinear phenomena in wave theory and marine hydrodynamics", *Applied Ocean Research*, vol. 24, pp. 261-274, 2002.

[17] B.F. Ronalds, Y.T. Wong, S. Tuty & E.J. Piermattei, "Monopod reliability offshore Australia", *Proc. 17th Int. Conf. OMAE*, ASME, Lisbon, 1998.